Molecular Therapy
Methods & Clinical Development
Original Article

Generation and GMP scale-up of human CAR-T cells using non-viral *Sleeping Beauty* transposons for B cell malignances

Begoña Diez,[1,2,3,15] Cristina Calviño,[4,15] María Fernández-García,[1,2,3] Paula Rodríguez-Márquez,[5] Saray Rodríguez-Díaz,[5] Rebeca Martínez-Turillas,[5,7] Candela Ceballos,[8] Jorge Illarramendi,[8] Juana Serrano-López,[9] Csaba Miskey,[10] Almudena Navarro-Bailón,[7,11,12] Lucía López-Corral,[7,11,12] Pilar Llamas,[9,13] Margarita Redondo,[8] Fermín Sánchez-Guijo,[7,11,12] Jose Rifon,[4,6,7] Ana Alfonso-Piérola,[4,6,7] Zoltán Ivics,[10] Susana Inogés,[4,6,7] Ascensión López-Díaz de Cerio,[4,6,7] Rosa Yanez,[1,2,3] Juan A. Bueren,[1,2,3,14] Juan R. Rodríguez-Madoz,[5,6,7,14] and Felipe Prosper[4,5,6,7,14]

[1]Hematopoietic Innovative Therapies Division, Centro de Investigaciones Energeticas Medioambientales y Tecnologicas (CIEMAT), Madrid, Spain; [2]Advanced Therapies Unit, IIS Fundación Jimenez Diaz, Universidad Autonoma de Madrid, Madrid, Spain; [3]Biomedical Research Network Center on Rare Diseases (CIBERER), Madrid, Spain; [4]Hematology and Cell Therapy Department, Clinica Universidad de Navarra (CUN), IdiSNA, Pamplona, Spain; [5]Hemato-Oncology Program, Cancer Division, Cima Universidad de Navarra, IdiSNA, Pamplona, Spain; [6]Cancer Center Clinica Universidad de Navarra (CCUN), Pamplona, Spain; [7]Biomedical Research Network Center on Cancer (CIBERONC), Madrid, Spain; [8]Servicio de Hematología, Hospital Universitario de Navarra, IdiSNA, Pamplona, Spain; [9]Experimental Hematology Lab, IIS-Fundacion Jimenez Díaz, UAM, Madrid, Spain; [10]Transposition and Genome Engineering, Division of Hematology, Cell and Gene Therapy, Paul Ehrlich Institute, Langen, Germany; [11]Hematology Department, IBSAL-University Hospital of Salamanca, Salamanca, Spain; [12]Center for Cancer Research (CIC-IBMCC) and Department of Medicine, University of Salamanca, Salamanca, Spain; [13]Hematology Department, Fundacion Jiménez Diaz University Hospital, Madrid, Spain

Most CAR-T therapies rely on genetic T cell engineering with integrating viral vectors that, although effective, are associated with prohibitive costs. Here we have generated TranspoCART19 cells, a fully functional 4-1BB second-generation CAR-T cell product targeting CD19, fused to a truncated version of the human EGFR (hEGFRt) as reporter gene and safety switch, based on the *Sleeping Beauty* transposon delivery system. Our manufacturing protocol allowed generation of TranspoCART19 cells under GMP conditions, showing similar *in vitro* and *in vivo* antitumoral efficacy than conventional CAR-T cells generated with lentiviral vectors. Additionally, membrane expression of hEGFRt facilitated *in vivo* CAR-T cell elimination after cetuximab administration. Safety analyses showed that TranspoCART19 cells presented low vector copy numbers and close-to-random vector integration profiles. Moreover, final TranspoCART19 products lacked non-integrated genomic material used for the generation of CAR-T cells and were free from transposase protein. *In vivo* biodistribution analyses revealed that TranspoCART19 cells were mainly present in hematopoietic organs with no gender bias. Altogether, this study provides a cost-effective, GMP-compliant manufacturing process for the generation of CAR-T cells using non-viral vectors. These results have supported the approval of a clinical trial to evaluate TranspoCART19 cells in patients with relapsed/refractory lymphoma (NCT06378190) that is currently ongoing.

INTRODUCTION

Immunotherapy using chimeric antigen receptor (CAR) T cells has shown great efficiency for the treatment of several hematological malignances, such as B cell leukemia, lymphoma, and multiple myeloma.[1] Due to their proven efficacy in the clinic, several CAR-T cell products have been approved both in the United States and in Europe and are already available as commercial advanced therapy medicinal products (ATMPs) in several countries.[2–9] Despite their remarkable efficacy, CAR-T therapies still present a number of limitations, some of them derived from the elevated costs of gamma-retroviral (RV) or lentiviral vectors (LVs) used for T cell engineering, and also some malignant transformation concerns.[10–13] While the final cost of CAR-T therapies is multifactorial,[14] their use for the treatment of diseases with a relatively high prevalence will require the treatment of a large number of patients, implying a significant burden for National Health Systems.

To minimize costs of viral vector-based CAR-T cells, the use of non-viral vectors, such as transposon systems, has been largely pursued.[15]

Received 15 October 2024; accepted 28 January 2025;
https://doi.org/10.1016/j.omtm.2025.101425.

[14]Senior author

[15]These authors contributed equally

Correspondence: Juan A. Bueren, Hematopoietic Innovative Therapies Division, Centro de Investigaciones Energeticas Medioambientales y Tecnologicas (CIEMAT), Madrid, Spain.
E-mail: juan.bueren@ciemat.es
Correspondence: Juan R. Rodríguez-Madoz, Hemato-Oncology Program, Cancer Division, Cima Universidad de Navarra, IdiSNA, Pamplona, Spain.
E-mail: jrrodriguez@unav.es
Correspondence: Felipe Prosper, Hematology and Cell Therapy Department, Clinica Universidad de Navarra (CUN), IdiSNA, Pamplona, Spain.
E-mail: fprosper@unav.es

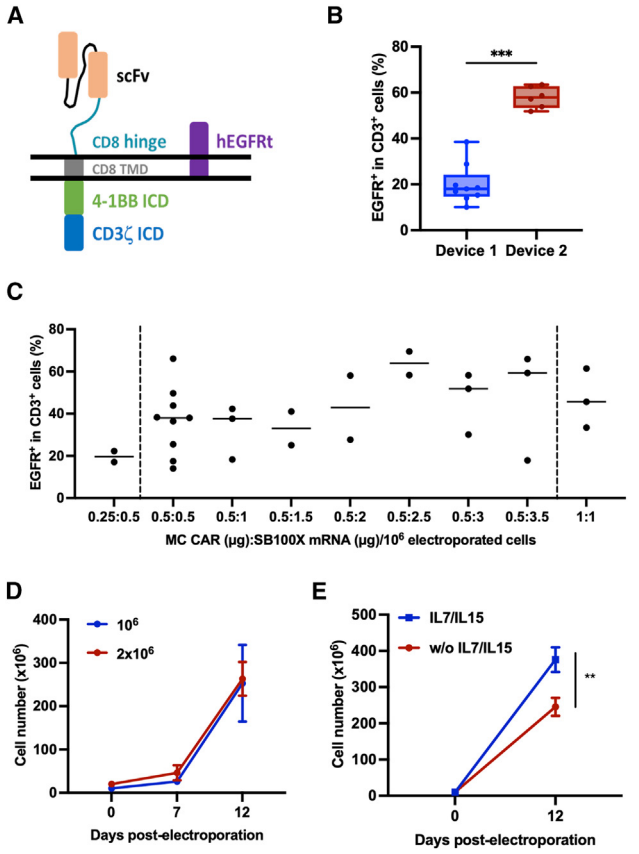

Figure 1. Optimization of TranspoCART19 cell production

(A) Schematic representation of the TranspoCART19 construct, a 4-1BB second-generation construct targeting CD19, fused to a truncated version of the human EGFR (hEGFRt) as a reporter gene and safety switch. (B) Transfection efficiency ($EGFR^+$ cells) of primary T cells 14 days after electroporation with MC expressing CAR and SB100X mRNA. Two different electroporation devices were used. D1: Lonza 4D-Nucleofector System (n = 9). D2: MaxCyte ExPERT GTx Flow Transfection System electroporator (n = 6). Graph represents mean and 25 and 75 percentiles and SD. (C) Transfection efficiency at 14 days after T cell electroporation using different MC:mRNA ratios on D2. (D) Evaluation of TranspoCART19 cells expansion at two different seeding densities (10^6 and 2×10^6 cells/cm^2) in the P-6M G-Rex bioreactors. Graph represents the mean ± SD (n = 3). (E) Evaluation of TranspoCART19 cells expansion in the presence/absence of cytokines (IL-7 and IL-15) added at the middle of the expansion period. Graph represents the mean ± SD (n = 2). Unpaired t test (B), two-way ANOVA with Tukey's multiple comparisons test (D and E). ns: not significant; *$p < 0.05$; **$p < 0.01$, ***$p < 0.001$.

Like viral vectors, transposon systems can integrate exogenous DNA in the genome when these constructs are electroporated together with the specific transposase in target cells.[16] In contrast to viral vectors, the GMP manufacturing of the transposon DNA and the transposase—frequently used as an mRNA molecule—is much simpler and less expensive. Consequently, further research is essential to develop optimal CAR-T cell products that meet the standards of safety and efficacy matched with cost-effective manufacturing. Additionally, transposon systems also have a larger cargo capacity compared with RVs and LVs. Several types of transposons have been already used in clinical trials to manufacture CAR-T cell products, such us *piggyBac* (PB) and *Sleeping Beauty* (SB) transposon systems. However, recent studies have reported serious adverse effects in two patients treated with CAR-T cell-generated with PB-based systems,[11–13] probably due genotoxic events related to the integration profile, similar to the ones described for RVs.[17] In contrast, previous studies in CAR-T cells generated with SB-based transposon systems strongly suggest the safety of these non-viral vectors due to their close-to-random integration profile, thus with no integration preference for transcription start sites nor coding sequences.[18–21] This safer profile, together with the simplified manufacturing that SB-transposon systems present over viral vectors, represent a valuable tool for the generation of cost-effective CAR-T cell products for clinical purposes.

In the present study, we report the generation of TranspoCART19 cells, an SB-transposon based CAR-T cell product that targets the CD19 antigen, fused to a truncated epidermal growth factor receptor (hEGFRt) as a reporter gene and a safety switch. We report the optimized cost-effective and reproducible GMP-grade manufacturing process, as well as the pre-clinical safety and antitumoral efficacy of these cells.

RESULTS

Optimization of TranspoCART19 cell production

We optimized the generation of CAR-T cells using the *Sleeping Beauty* transposon system, to deliver a 4-1BB second-generation CAR construct that targets the CD19 antigen. The CAR coding sequence was fused to a truncated version of the human EGFR (hEGFRt) as a reporter gene, to facilitate tracking of CAR-T cells, and as a safety switch, allowing CAR-T cell depletion when required (Figures 1A and S1). The similar co-expression levels of the hEGFRt and the CAR on the membrane of transfected T cells was confirmed by flow cytometry in different samples from healthy donors (Figure S1). To optimize the conditions for the generation of CAR-T cells (TranspoCART19 cells), the transposon vector was used as minicircle (MC) and the SB100X transposase was provided as mRNA to transduce purified $CD4^+$ and $CD8^+$ T cells from healthy donor peripheral blood samples, as described in the materials and methods. Different GMP-compatible electroporation systems were evaluated for MC and mRNA delivery, analyzing the percentage of hEGFRt in the membrane of the modified T cells as a surrogate indicator of the transfection efficacy, and the MaxCyte ExPERT GTx was selected since higher transfection rates with lower variability were obtained (Figure 1B). We optimized the MC and mRNA ratio that provided high transfection efficiency with better viability and recovery of the cells after electroporation. A concentration of 0.5 µg of MC and 0.5 µg of SB100X mRNA per 10^6 cells was selected, as different ratios with higher amounts of MC:mRNA were able to increase the transduction efficiency up to 70% but at the expense of a reduction in cell recovery (Figures 1C and S1). In addition, the use of different cell concentrations at the initiation of the culture (10^6 and 2×10^6 cells/cm^2) generated the same number of CAR^+ cells at the end of the expansion (Figures 1D and S1). Finally, the addition of cytokines (interleukin [IL]-7 and IL-15) significantly improved the cell

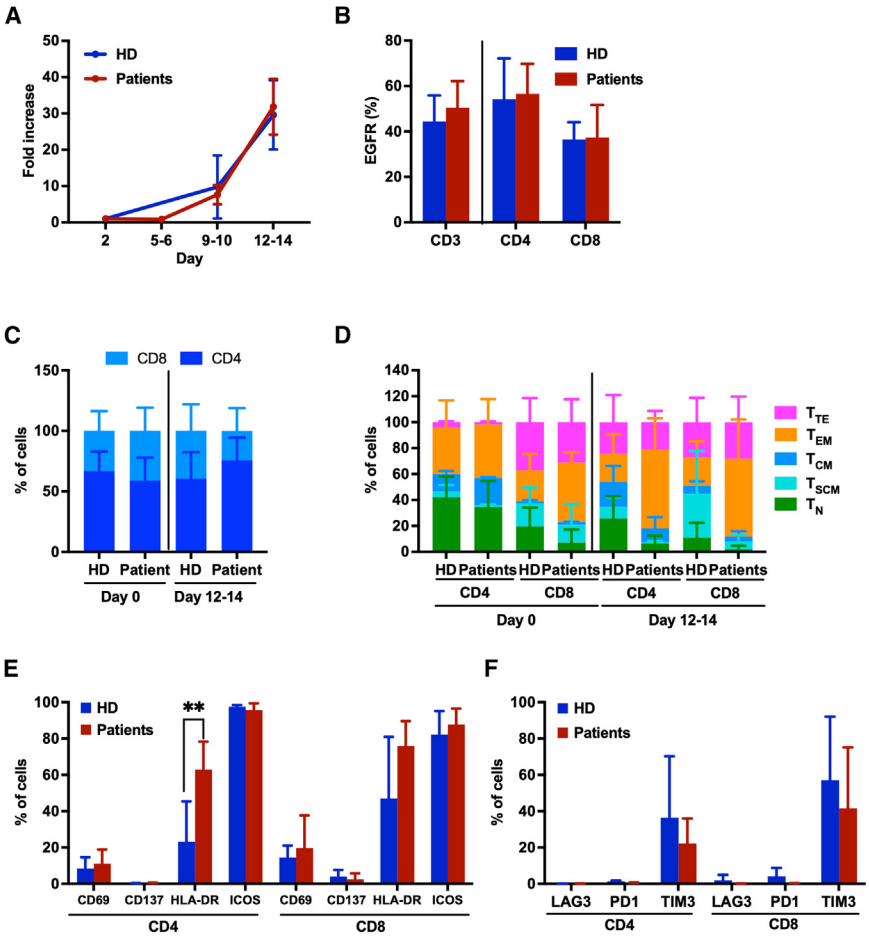

Figure 2. Phenotypic characterization of TranspoCART19 cells

(A) Expansion of TranspoCART19 cells generated from three patients with different CD19$^+$ malignancies (two ALL and one DLBCL) and four healthy donors (HD) during CAR-T cell production. (B) Percentage of transduced cells at the end of TranspoCART19 cell production. Graph represents the percentage of CAR$^+$ cells (EGFR$^+$) in different lymphocyte subpopulations in HD and patients. (C) Analysis of CD4/CD8 ratio in basal T cells (day 0) and TranspoCART19 cells at end of expansion period (day 12–14) in HDs and patients. (D) Analysis of the phenotype of basal T cells (day 0) and TranspoCART19 cells at end of expansion period (day 12–14) in HDs and patients. CAR-T cell subpopulations within CD4$^+$ and CD8$^+$ cells are depicted. T_N: naive; T_{SCM}: stem central memory; T_{CM}: central memory; T_{EM}: effector memory; T_E: effector. (E) Analysis of the expression of activation marker (CD69, CD137, HLA-DR, and ICOS) in TranspoCART19 cells from HDs and patients at end of expansion period (days 12–14). (F) Analysis of the expression of inhibition marker (LAG3, PD1 and TIM3) in TranspoCART19 cells from HDs and patients at end of the expansion period (days 12–14). Mean ± SD for each group is depicted. two-way ANOVA with Tukey's multiple comparisons test (A, B, C, E, and F). ns: not significant; $^*p < 0.05$; $^{**}p < 0.01$, $^{***}p < 0.001$.

expansion without an impact on the percentage of CAR$^+$ cells (Figure 1E). According to these results, cells were expanded at a seeding density of 10^6 cells/cm^2 in the presence of IL-7 and IL-15.

Phenotypic and functional characterization of TranspoCART19 cells

Once electroporation and expansion conditions compatible with clinical scale CAR-T cell production had been optimized, TranspoCART19 cells were phenotypically and functionally characterized using PB from four healthy donors (HDs) and three patients with different CD19$^+$ malignancies (two acute lymphoblastic leukemia [ALL] and one diffuse large B cell lymphoma [DLBCL]). We did not find significant differences in the fold expansion between cells from HD and patients with B cell malignancies, and also a similar percentage of CAR-T cells was observed in these two groups (Figures 2A and S2). Overall, a slightly higher proportion of CAR-T cells was observed in the CD4$^+$ population in comparison with CD8$^+$ cells (Figure 2B). Distribution of CD4$^+$ and CD8$^+$ subpopulations before and after TranspoCART19 manufacturing was also similar with no differences between HD and patients (Figure 2C). Phenotypic analysis of the T cell subpopulations revealed similar distribution of the different populations between HD and patients at baseline levels. However, TranspoCART19 cells generated from patient samples presented a more differentiated phenotype with higher percentage of effector memory T cells in both CD4$^+$ and CD8$^+$ subpopulations (Figure 2D). The presence of several activation (CD69, CD137, HLA-DR, and ICOS) and exhaustion (LAG3, PD1, and TIM3) markers was also analyzed in the TranspoCART19 cells to determine the status of the final product (Figures 2E and 2F). High expression of HLA-DR and ICOS was observed in both CD4$^+$ and CD8$^+$ subpopulations with increased proportion of HLA-DR-positive cells in CD4$^+$ cells from patients. CD69, CD137, PD1, and LAG3 expression was barely detected in the final products. However, TIM3 was moderately expressed in TranspoCART19 cells from both HD and patients, probably due to the active state of the cells rather than a sign of exhaustion.

Functional characterization was first assessed in *in vitro* studies, measuring the cytotoxic activity and cytokine production of TranspoCART19 cells against CD19$^+$ tumoral cells. CAR-T cells from both HDs and patients showed a very high and specific cytotoxic effect at low E/T ratios against CD19$^+$ expressing tumor cell lines and primary cells (Figures 3A and S3). Moreover, the production of proinflammatory cytokines (interferon [IFN]γ, IL-2, tumor necrosis factor [TNFα], and IL-4) by CAR-T cells, as measured with Legend Plex HU Essential Immune Response Panel, was only detected in cultures with CD19$^+$ expressing tumor cells, corroborating the specificity of the TranspoCART19 cell product (Figures 3B and

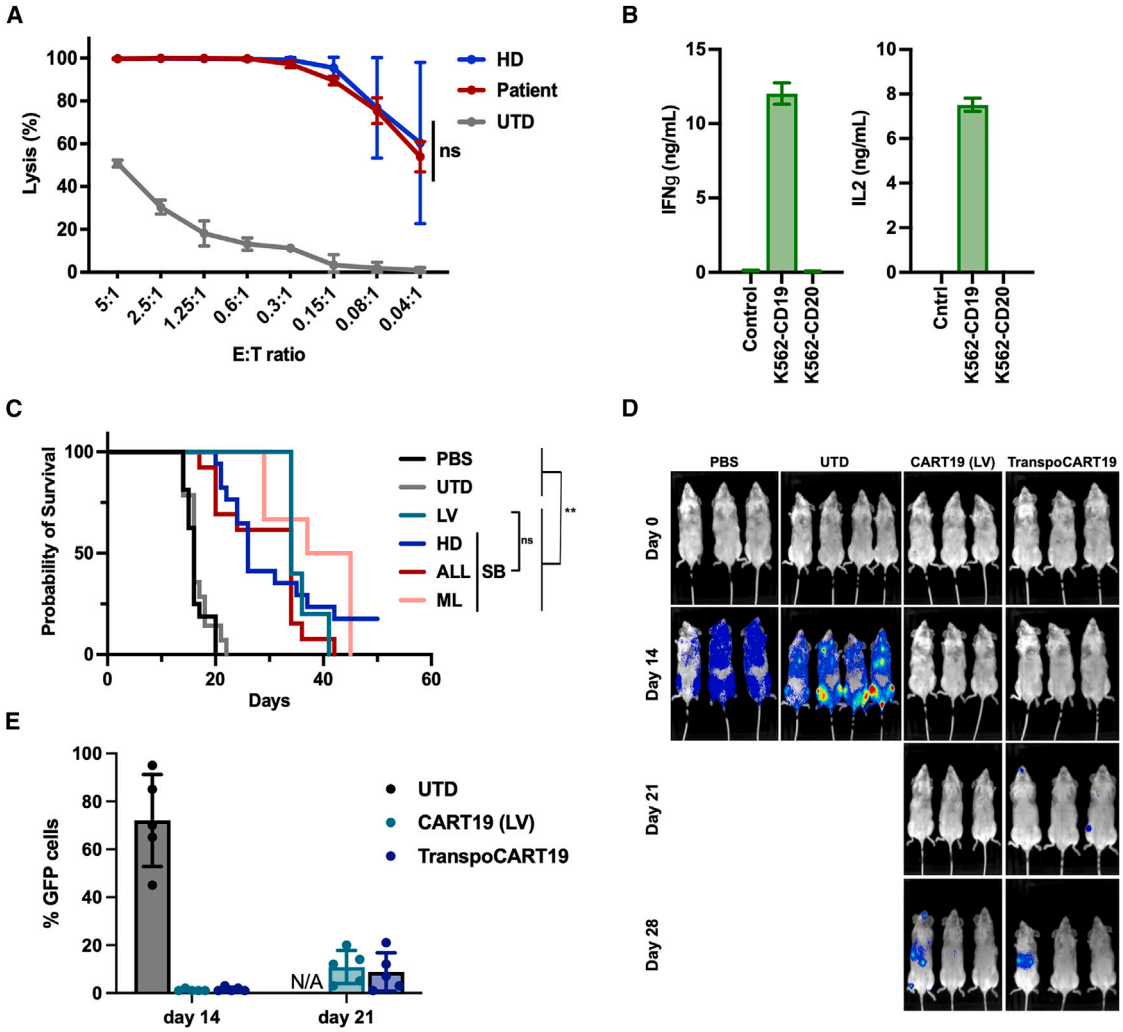

Figure 3. Functional characterization of TranspoCART19 cells

(A) Quantification of the cytotoxic activity of TranspoCART19 cells generated from HD ($n = 4$) and patients ($n = 3$), against CD19$^+$ tumoral cell line NALM6 at different E:T ratio. The percentage of specific lysis for each CAR-T cell production is depicted. (B) Quantification of IFN-γ and IL-2 levels in supernatants from cytotoxic assays measured by ELISA. (C) Survival of mice treated with TranspoCART19 cells from HDs ($n = 17$) or ALL ($n = 13$) or ML patients ($n = 6$). Untreated animals ($n = 16$), treated with UTD cells ($n = 14$) or with CAR-T cells produced with lentiviral vectors (LVs, $n = 5$) were use as controls. (D) Bioluminescence analysis of animals treated with TranspoCART19 cells or with CAR-T cells produced with lentiviral vectors (CART19-LVs), both from healthy donors. Untreated animals (PBS) or treated with untransduced (UTD) cells were used as control. Bioluminescence images were acquired at indicated time points after treatment. (E) Quantification of NALM6 tumoral cells (GFP) at different times after CAR-T cell administration by flow cytometry. Two-way ANOVA with Tukey's multiple comparisons test (A). Log rank (Mantel-Cox) test (D). ns: not significant; *$p < 0.05$; **$p < 0.01$, ***$p < 0.001$.

S3). Finally, the *in vivo* antitumoral efficacy of TranspoCART19 cells was evaluated in a xenograft model in NSG mice by administration of 3×10^6 CAR-T cells/animal, 3 days after the intravenous administration of 1×10^6 luciferase-expressing NALM6 cells per animal. TranspoCART19 cells acquired a more differentiated phenotype after infusion, with increased proportions of effector memory and terminally differentiated effector cells in both CD4 and CD8 compartments. These results are in accordance with our previous observations with similar CAR-T constructs targeting different antigens (BCMA or CD33),[22,23] showing that at the peak of expansion, most CAR-T cells acquire an effector memory phenotype (Figure S3). The survival of mice treated with LV and SB-transposon-based CAR-T cells was compared with mice treated with untransduced T cells (UTD) or with (PBS). TranspoCART19 cells from either HD and from patients with different types of CD19$^+$ tumors increased the survival of the animals in comparison with UTD and PBS controls, and achieved similar efficacies, with no statistical differences ($p = 0.3415$), when compared with CD19 CAR-T cells generated with LV (Figure 3C). Moreover, a clear reduction of the tumor burden was observed at different days after CAR-T cell

infusion by both bioluminescence analysis as well as quantification of tumoral cells (Figures 3D and 3E).

Manufacturing and characterization of clinical-grade TranspoCART19 cells

In order to scale-up the production of TranspoCART19 cells, a preclinical large-scale production was performed in two different laboratories, starting from the same fresh sample from a healthy donor. Thus, 100×10^6 of activated T cells were electroporated using the optimized conditions (0.5:0.5 μg of MC:mRNA) in the MaxCyte ExPERT GTx electroporation system and were expanded for 11 days in G-Rex bioreactors, refeeding the cultures with fresh cytokines on day 5. At the end of the expansion period, cells were harvested, washed, and formulated for cryopreservation. We observed similar growth and expansion rates in both facilities, and similar percentages of CAR-T cells and phenotypic characteristics in both $CD4^+$ and $CD8^+$ T cell subpopulations (Figures 4A–4D). Regarding the activation markers, the final CAR-T cell products presented high expression of ICOS and HLA-DR, meanwhile TIM3 was the unique inhibitory marker present in the final products (Figures 4E and 4F). The cytotoxicity activity against a $CD19^+$ was also similar with slight differences at very low ratios (Figure 4G).

Finally, the GMP production of TranspoCART19 cells, using fresh and frozen leukapheresis as starting materials, was validated in both facilities. Thus, leukapheresis samples from two HDs were divided into two equal parts that were processed in each laboratory, as described in the materials and methods. Again, 100×10^6 of activated T cells were electroporated and expanded for 11 days according to the optimized conditions described above. A median expansion rate of 38.7 times (36.2–40.7) was obtained in the four validations, reaching an average of 3.9×10^9 total cells at the end of the incubation period. Moreover, the median proportion of CAR-T cells in all productions was 60.2% (55.5–65.8) with cell viabilities over 85%, resulting in a total number of $2.1–2.6 \times 10^9$ TranspoCART19 cells. In terms of functionality, the four productions presented >90% of cytotoxic activity against NALM6 cells at an E:T ratio of 2.5:1. Finally, all TranspoCART19 final products were sterile, endotoxin- and mycoplasma-free, translucent, and without aggregates. All the characteristics are summarized in Table 1. These results corroborated that the manufacturing process is robust from either fresh or frozen leukapheresis, with no differences related to the starting material and similar characteristics between facilities, obtaining TranspoCART19 products fulfilling all the release criteria stablished for the clinical trial.

Safety analysis of TranspoCART19 cells

To determine the safety profile of TranspoCART19 cells, vector copy numbers (VCNs)/cell and insertion site analyses (ISAs) were performed using genomic DNA from four TranspoCART19 cell productions. We observed that all TranspoCART19 cell products analyzed presented a mean value of 5.16 copies/cell, lower than the 15 copies/cell limit established among the release criteria (Figure 5A; Table 1). Then, we performed ISA analysis, to map and characterize unique insertion sites of our TranspoCART19 cells. Results revealed that all insertions occurred into AT-rich DNA regions with the canonical palindromic ATATATAT motif containing the already described TA dinucleotide consensus target sequence of SB,[20] adjacent to the insertion site (Figure S4). We further analyzed whether there was a preference of insertions into distinct genomic sites, including exons, introns, gene bodies, and cancer-related genes. We found that insertions in our TranspoCART19 cells occurred in a close-to-random distribution, showing only a 1.4-fold enrichment in cancer-related genes and a 1.25-fold enrichment in exons (0.8-fold in coding exons) relative to the expected random frequency. In contrast, LV-associated insertions used as control presented a significantly higher enrichment in these categories (2.66-fold in cancer genes, 2.1-fold in exons, and 2.86-fold in coding exons) (Figure 5B). Moreover, when focusing on integrations at genomic safe harbor (GSH) sites, we observed significantly increased proportions in TranspoCART19 cells compared with LV-based CAR-T cells (Figures 5C and S4). Next, we analyzed whether TranspoCART19 cell products were free of transposase protein and non-integrated MC. Western blot analysis revealed that transposase protein was only detectable during the first 5 days of the expansion being undetectable from day 7 onward. Similarly, qPCR analysis showed that non-integrated MC was diluted during CAR-T cell expansion, being undetectable in the final product (Figures 5D and 5E). These results corroborate that our TranspoCART19 cell products lack the genomic material used for their generation.

One of the design features of TranspoCART19 cells is the presence of a hEGFRt on the membrane of transduced T cells to act as both a reporter gene and a safety switch. Thus, we evaluated the anti-EGFR-mediated CAR-T cell depletion efficacy *in vivo*. Mice were injected with TranspoCART19 cells, and a group of mice was treated with cetuximab, an approved anti-EGFR antibody used in the clinic (Figure 6A). Mice treated with a control antibody and mice without TranspoCART19 cells were used as control. FACS analysis of blood samples at different times after cetuximab administration revealed an efficient elimination of transplanted human T cells (Figure 6B), confirming the functionality of the safety switch. In addition, although some degree of recovery of $CD45^+CD3^+$ cells after cetuximab withdrawal was observed, this was very limited, with only one out of five animals presenting relevant levels of T cells (Figure S5). Moreover, at day 15, the percentage of cells expressing the CAR within those $CD45^+CD3^+$ in the animal receiving cetuximab was further decreased in comparison with the levels observed in control animals (Figure 6C). Finally, biodistribution studies were performed to evaluate the localization of TranspoCART19 cells after infusion. We observed increasing numbers of human $CD45^+$ cells mainly in the hematopoietic organs of the treated mice, such as bone marrow, peripheral blood, and spleen, being similar between male and female animals, indicting no gender bias. However, reduced but still detectable levels were observed in lung and liver during the 21 days of study (Figures 6D and S5). These results were also corroborated by measuring the VCN on these organs (Figure S5). Taken together, all these results would ensure the safety of TranspoCART19 cell product in the forthcoming clinical trial application.

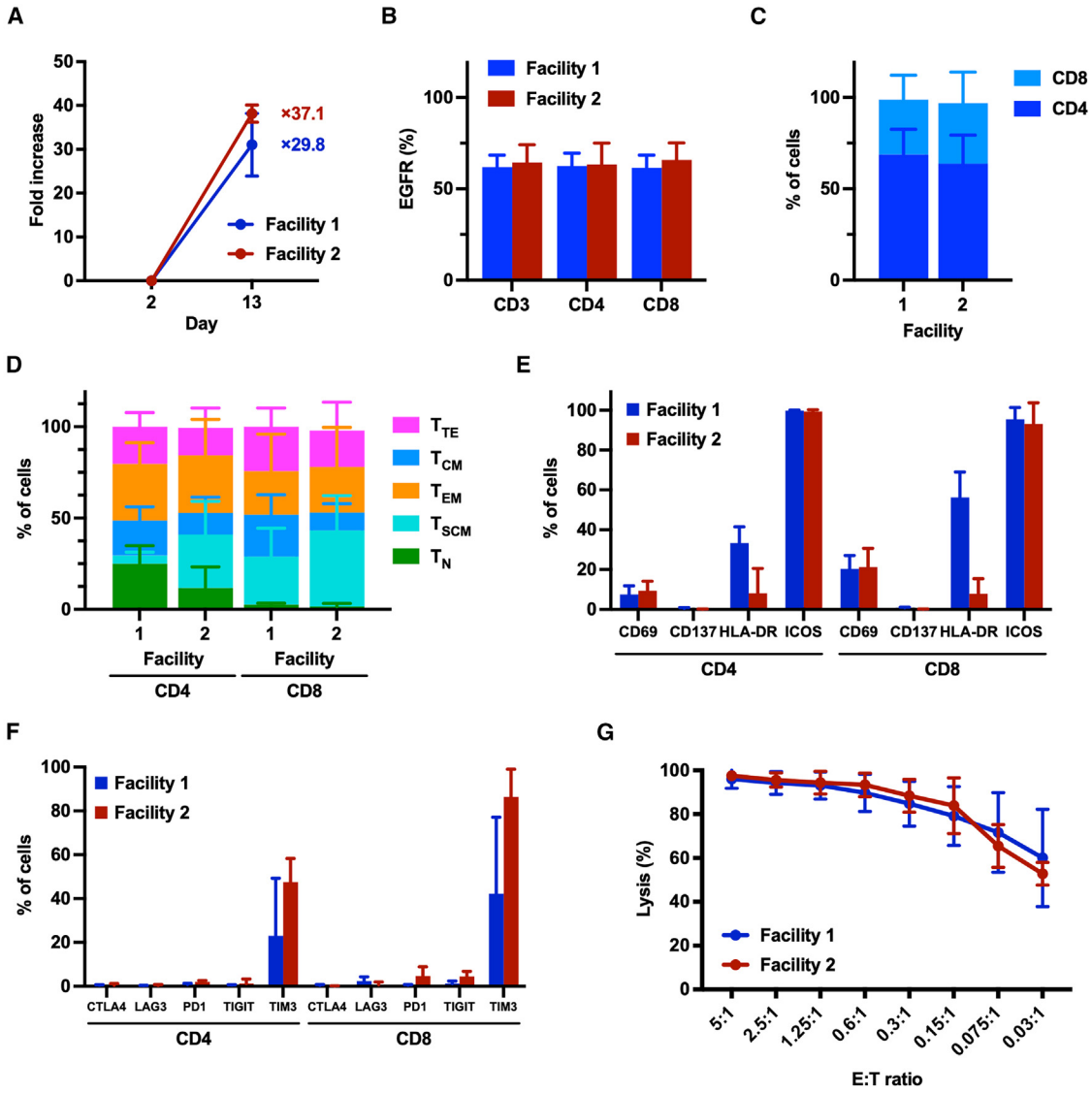

Figure 4. Characterization of pre-clinical large-scale pTranspoCART19 cell production

Large-scale TranspoCART19 production was performed in two different facilities starting from the same fresh sample from an HD (n = 3 each). (A) Evaluation of TranspoCART19 cell expansion at 11 days after electroporation. (B) Percentage of transduced cells at the end of TranspoCART19 cell productions. Graph represents the percentage of CAR^+ cells ($EGFR^+$) in different lymphocyte subpopulations. (C) Analysis of CD4/CD8 ratio in TranspoCART19 cells at end of expansion period. (D) Analysis of the phenotype of TranspoCART19 cells at end of expansion period. CAR-T cell subpopulations within $CD4^+$ and $CD8^+$ cells are depicted. T_N: naive; T_{SCM}: stem central memory; T_{CM}: central memory; T_{EM}: effector memory; T_E: effector. (E) Analysis of the expression of activation marker (CD69, CD137, HLA-DR, and ICOS) in TranspoCART19 cells at end of the expansion period. (F) Analysis of the expression of inhibition marker (CTLA-4, LAG3, PD1, TIGIT, and TIM3) in TranspoCART19 cells at end of the expansion period. (G) Quantification of the cytotoxic activity of TranspoCART19 cells against $CD19^+$ tumoral cell line NALM6 at different E:T ratio. The percentage of specific lysis for each CAR-T cell production is depicted.

DISCUSSION

The infusion of CAR-T cells recognizing specific antigens expressed in cancer cells represent a therapeutic innovation for cancer treatment, with particularly relevant results in hematological malignancies, where clinical results have led to the approval of several CAR-T cell products.[2–9] Currently, the generation of CAR-T cells mostly relies on genetic engineering with integrating viral vectors that, although effective, present a number of limitations due to the complexity and high costs associated to the generation of these vectors.[14] In this respect, the dissemination of CAR-T therapies to diseases with relatively high prevalence will require the treatment of large number of patients. This will be particularly the case once CAR-T therapies show efficacy in solid tumors, implying serious concerns for National Health Authorities due to the elevated production

Table 1. Characterization of clinical-grade TranspoCART19 cells

		Fresh leukapheresis		Cryopreserved leukapheresis	
Attribute	Specification	Facility 1	Facility 2	Facility 1	Facility 2
Appearance	Translucent solution without aggregates	Translucent solution without aggregates	Translucent solution without aggregates	Translucent solution without aggregates	Translucent solution without aggregates
No. CAR-T cells	$\geq 1–5 \times 10^6$/kg	2.5×10^9	2.1×10^9	2.1×10^9	2.6×10^9
EGFR, %	≥15	61.4	58	55.5	65.8
Viability, %	≥70	96	94.3	91.8	86.6
CD3, %	≥70	94.8	94.4	98.8	95.5
Lysis (E:T ratio 2.5:1), %	≥50	100	97.41	92.72	98.61
Sterility	No micro-organism detection	Not detected	Not detected	Not detected	Not detected
Endotoxin	≤8.3 UE/mL	<0.03 UE/mL	1.03 UE/mL	<0.03 UE/mL	<0.5 UE/mL
Mycoplasma	Negative	Negative	Negative	Negative	Negative
Adventitious virus	Negative	Negative	Negative	Negative	Negative
VCN	≤15	5.05	3.51	6.05	6.21

costs. Consequently, further research is essential to develop CAR-T cell products that meet the standards of safety and efficacy using cost-effective manufacturing processes. Compared with viral vector systems, the use of Sleeping Beauty (SB) transposon minicircles combined with the corresponding mRNA transposase offers several advantages in terms of cost and scalability,[21,24] since their use eliminates the need for large-scale virus production.[25] Remarkably, estimated costs associated with DNA manufacturing for CAR-T cell production with transposon-based vectors represent around 10% of the direct costs associated with LV manufacturing,[21,26] offering a very significant advantage for the generation of CAR-T cells for clinical purposes. Moreover, SB-based systems, combined with genome editing technologies, would also represent valuable tools for the generation of universal off-the-shelf CAR-T cell approaches, currently under development.[22,27]

The current work was conceived to bring an innovative and cost-effective CAR-T cell product to the clinic. The TranspoCART19 product combines SB-transposon-based systems to generate multifunctional modular CAR designs with enhanced safety and optimized GMP-compliant production protocols fulfilling all regulatory requirements, which would overcome some of the limitations observed in the current CAR-T therapies. Previous pre-clinical and clinical studies have shown that transposons constitute efficient non-viral vectors to generate CAR-T cells using different CAR constructs.[22,24,27,28] Our optimized protocol, based on the electroporation of the SB-transposon system, followed by the cell expansion in G-Rex bioreactors, allows the generation of fully functional TranspoCART19 cells from patient samples that present similar *in vitro* and *in vivo* antitumoral efficacy than conventional CAR-T cells generated with LV vectors.[21] Moreover, we have also scaled-up and validated an optimized protocol to produce TranspoCART19 cells from fresh and frozen samples, under GMP conditions in two different GMP facilities. All the productions met the release criteria established for clinical application, indicating not only the scalability and reproducibility of the protocol but also the possibility to start from frozen leukapheresis. Importantly, although SB-transposon systems are still not widely used in clinical trials, the TranspoCART19 cells generated under GMP conditions were fully functional and showed phenotypic and functional characteristics comparable with CAR-T products generated for other clinical trials, like the CARAMBA trial.[24] Although CAR-T cells generated for the CARAMBA trial used a different CAR construct (targeting SLAMF7) to treat a different disease (multiple myeloma), and despite variations in the production protocol (separate CD4/D8 production vs. combined generation and different electroporation device), CAR-T cells generated in the CARAMBA trial presented equivalent features compared with the TranspoCART19 cells generated in the current study. However, according to recent publications,[29–31] the impact of the CD4/CD8 ratio, at least in CD19 targeting CAR-T cells, should be an aspect further evaluated.

In terms of safety, the VCNs/cell of all the TranspoCART19 cell productions was below the specification limit of 15 copies per cell, indicating that achieving high levels of transfection and CAR expression with reduced number of integrations is feasible, increasing the safety of the cell product. In addition, in contrast to RVs, LVs, and even other transposon vectors including PB, we observed a close-to-random integration profile, as it has been already documented for SB-based vectors,[19,24] corroborating the safer integration pattern in the genome of transfected cells, a fact that should reduce the risk of malignant transformation. These results would represent a key advantage over other transposon systems, including PB, due to the adverse events (i.e., development of lymphomas in patients treated with PB-modified CAR-T cells) recently reported.[11–13] Although the etiology of these lymphomas is still unclear,[11] it has been postulated that it could be related to the integration profile of PB-transposons, similar to that corresponding the genotoxic RVs. Moreover,

TranspoCART19 cells were also free from transposase protein or non-inserted minicircles at the end of the manufacturing process. Additionally, the functionality of the safety switch inducing a fast depletion of TranspoCART19 cells, upon cetuximab administration, was clearly demonstrated. Although some degree of recovery of TranspoCART19 cells after cetuximab withdrawal can be observed, this was very limited, with only one out of five animals presenting relevant levels of $CD45^+CD3^+$ cells. In addition, in this particular animal only 30.2% of $CD45^+CD3^+$ cells expressed the CAR. This small proportion of persisting CAR-T cells could be eliminated with longer administrations of cetuximab. Moreover, translation of cetuximab administration to a clinical setting is an aspect that should be further optimized to achieve full and fast depletion of TranspoCART19 cells. Finally, biodistribution studies in mice infused with these cells evidenced the absence of TranspoCART19 cells and/or genetic material in gonads or other tissues rather than hematopoietic organs, increasing our evidence about the safety of the product.

All in all, the results from our work have supported the approval by the Spanish Agency of Medicines and Medical Products (AEMPS) of an open-label, prospective, multicenter, and non-randomized Phase-I/IIa clinical trial (NCT06378190) to evaluate the feasibility of using TranspoCART19 cells as treatment for R/R B cell lymphomas, their safety (assessed by the number and severity of adverse events), and their antitumoral efficacy, that is currently ongoing. The study design comprising a classical 3 + 3 dose escalation phase (Phase I) with an additional expansion cohort (Phase IIa). During phase I, three different dose levels (DL) of TranspoCART19 cells, administered in three fractionated doses (10%, 30%, and 60%), are being evaluated (1×10^6 cells/kg, 3×10^6 cells/kg, and 5×10^6 cells/kg), with an accepted DL-1 of 0.5×10^6 cells/kg if serious adverse events are observed. Phase II, to evaluate efficacy, will be performed with the recommended phase II dose (RP2D) determined in phase I. TranspoCART19 cell production will be conducted at two GMP facilities, following the optimized procedures described in this work, which have been also approved by the AEMPS. Patients with diffuse large B cell lymphoma (DLBCL), primary central nervous system lymphoma (PCNSL), mantle cell lymphoma (MCL), follicular lymphoma (FL), or marginal zone B cell lymphoma (MZL), refractory or relapsed to at least two prior lines of systemic treatment are eligible for inclusion.

In conclusion, we have optimized a cost-effective and reproducible GMP-grade manufacturing process of TranspoCART19 cells, a CD19-targeting CAR-T cells that present fully functional characteristics and antitumoral efficacy, together with a safety profile. Altogether, our results have enabled us to obtain the approval for a clinical trial to evaluate the safety and efficacy of TranspoCART19 cells in R/R lymphoma patients (NCT06378190).

MATERIALS AND METHODS

Patient and healthy donor samples

Peripheral blood samples were obtained from HDs and patients with B hematological malignancies (four with acute lymphoblastic leukemia [ALL], three with diffuse large B cell lymphoma [DLBCL], two with follicular lymphoma [FL], and one with mantle cell lymphoma [MCL]). Sample collection was conducted in accordance with the principles of the Declaration of Helsinki and with the approval of the Research Ethical Committee of the University of Navarra, the Fundación Jiménez Díaz Hospital and the University Hospital of Salamanca. All subjects provided written informed consent.

Culture cell lines

Cell lines (K562, K562-CD20, K562-CD19, K562-CD19-luciferase, and NALM6-luciferase) were cultured in RPMI-1640 supplemented with 10% FBS, with 1% penicillin/streptomycin (Gibco) and 1% L-Glutamine (Gibco). All cell lines were maintained at 37°C in 5% CO_2. Primary tumoral cells were obtained from peripheral blood mononuclear cells (PBMCs) isolated by Ficoll-Paque density gradient centrifugation from patients with $CD19^+$ malignancies, including ALL and DLBCL. The percentage of $CD19^+$ cells was determined by flow cytometry (>90%) and cells were used directly for cytotoxicity assays.

Generation of CD19 targeting CAR construct and SB100X mRNA

The pT2/BH vector (gift from Perry Hackett; Addgene plasmid # 26556) was used to express under the EF1a promoter a second-generation CAR construct comprising the CD8a signal peptide, the single-chain variable fragment targeting CD19 (scFv from FMC63 clone), a CD8 hinge and transmembrane domain, and the 4-1BB and CD3ζ endodomains fused to a truncated version of the human EGFR (hEGFRt).[32] Minicircles (MCs) carrying the EF1a.19BBzE transposon were generated from parental pT2 plasmids by PlasmidFactory GmbH using site-specific recombination and purified by affinity chromatography. Polyadenylated (120A), capped (CleanCap AG), and modified (5-Methoxy-U) mRNA coding for a codon optimized version of the SB100X was derived from pCMV(CAT)T7-SB100 vector (gift from Zsuzsanna Izsvak; Addgene plasmid #34879), and synthesized by TriLink BioTechnologies.

TranspoCART19 cell generation

PBMCs were isolated from blood by Ficoll-Paque density gradient centrifugation. $CD4^+$ and $CD8^+$ T cells were selected using CD4 and CD8 MicroBeads (Miltenyi Biotec) in the AutoMACS Pro or CliniMACS Separator (Miltenyi Biotec) following the manufacturer's instructions. Isolated T cells, at the natural CD4/CD8 ratio present on the original sample, were activated with 10 μL/mL T cell TransAct (Miltenyi Biotec) for 48 h and then 2×10^6 activated T cells were electroporated with 0.5 μg of MC and 0.5 μg of SB100X mRNA using the Lonza 4D-Nucleofector System (D1) or the MaxCyte ExPERT GTx Flow Transfection System electroporator (D2), according to the manufacturer's instructions. To optimize the MC:mRNA ratio 2×10^6 activated T cells were electroporated with different conditions using the MaxCyte ExPERT GTx Flow Transfection System. Transposon-mediated CAR-T (TranspoCART19) cells were expanded in G-Rex devices (Willsonwolf) using TexMACS culture medium (Miltenyi Biotec) supplemented with 3% human serum (Sigma) and 625 IU/mL of human IL-7 (Miltenyi Biotec) and 85 IU/mL of IL-15

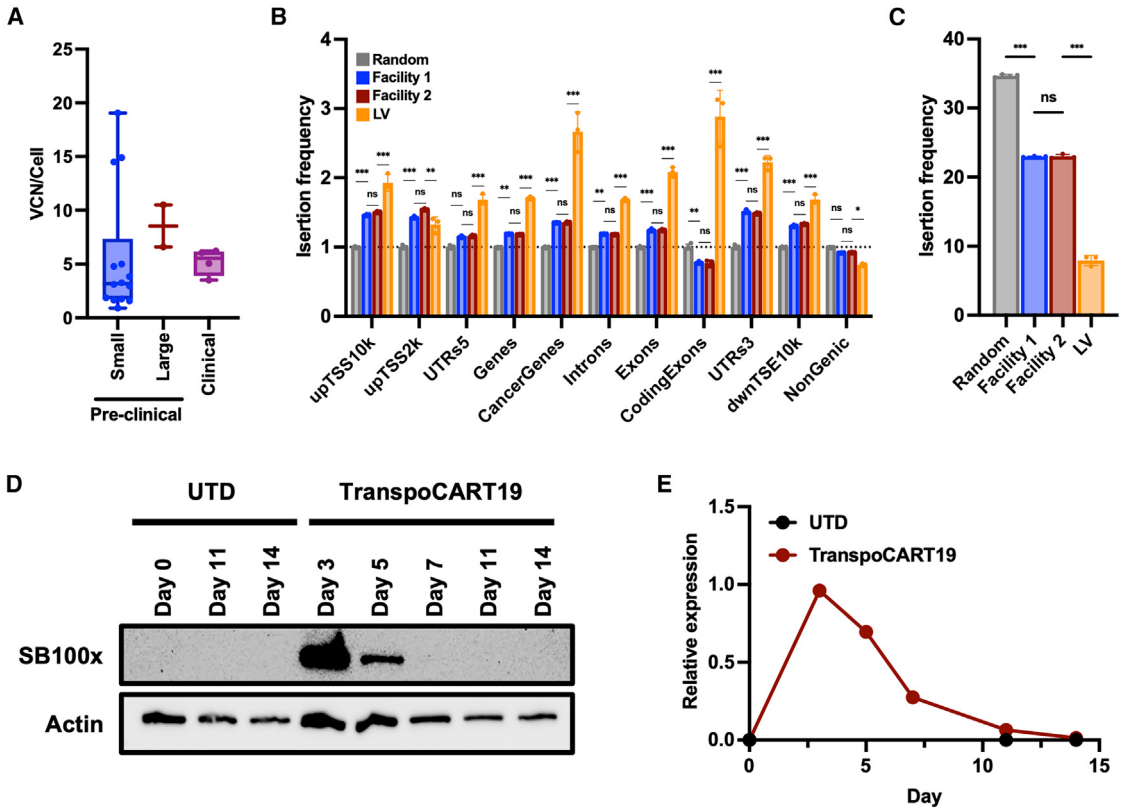

Figure 5. Safety analysis of TranspoCART19 cells

(A) Analysis of the vector copy number integrations in small pre-clinical (n = 14), large pre-clinical (n = 2) and clinical validations (n = 4) of TranspoCART19 productions. (B) Histogram plot showing the genomic distribution of vector integration sites in TranspoCART19 cells from pre-clinical large-scale validations produced in two different GMP facilities. Mean fold changes above the random expected insertion frequency (set to 1) are shown on the y axis. upTSS10k/upTSS2k: up to 10 or 2 kb upstream of transcriptional start sites, respectively; dwnTSE10k: up to 10 kb downstream of transcriptional end sites. (C) Histogram plot showing vector integration sites located at unified safe harbor categories in TranspoCART19 cells from pre-clinical large-scale validations. (D) Western blot analysis of SB100x transposase at different times during the manufacturing period of TranspoCART19 cells. UTD cells were used as controls. (E) Quantification of non-integrated MCs by qPCR at different times during the manufacturing period of TranspoCART19 cells. UTD cells were used as control. One-way ANOVA with Tukey's multiple comparisons test (A and C). Two-way ANOVA with Tukey's multiple comparisons test (B). ns: not significant; $*p < 0.05$; $**p < 0.01$, $***p < 0.001$.

(Miltenty Biotec). Seeding density was optimized in a G-Rex6M Well Plate, and finally, the expansion protocol was optimized in a G-Rex6M Well Plate evaluating the effect of cytokine addition on day 5 of the culture. After expansion (12–14 days), phenotypic and functional characterization of the cells was performed.

Scale-up and validation of the production protocol under GMP conditions

Scalation of TranspoCART19 cell production was performed in two GMP facilities using a healthy donor leukapheresis that was divided into two equal parts. CAR-T cells were generated following the optimized procedure described above scaling-up the reagents. Briefly, T cells were selected using CD4 and CD8 MicroBeads and 300×10^6 cells were activated with 10 µL/mL of Transact for 48 h. Subsequently, cells were harvested and 100×10^6 of T cells were electroporated with 0.5 µg/10^6 cells of CAR MC and 0.5 µg/10^6 cells of transposase mRNA using MaxCyte ExPERT GTx Flow Transfection System. After electroporation, cells were expanded for 11 days in G-Rex 100M device in 1,000 mL of TexMACS supplemented with 3% AB serum (ZKT Tubingen gGMbH), hIL-7 (625 IU/mL), and hIL-15 (87.5 IU/mL). After 5 days of culture, hIL-7 (625 IU/mL) and hIL-15 (87.5 IU/mL) were added. At the end of the expansion, TranspoCART19 cells were harvested for further experiments. Validations under GMP conditions were also conducted at each GMP facility using leukapheresis from two HDs divided into two equal parts. One leukapheresis was processed fresh, while the other was cryopreserved and used to validate the production from a frozen sample. CAR-T cells were generated using the protocol described above. After 11 days of culture, the cells were harvested for quality controls, including cell counting and viability assessment, CAR expression, phenotypic characterization, cytotoxic activity, VCN, and microbiological studies (detailed in the supplemental materials and methods). Aliquots of electroporated cells were cryopreserved in three fractions: 10%, 30%, and 60% of the total dose. All fractions were cryopreserved

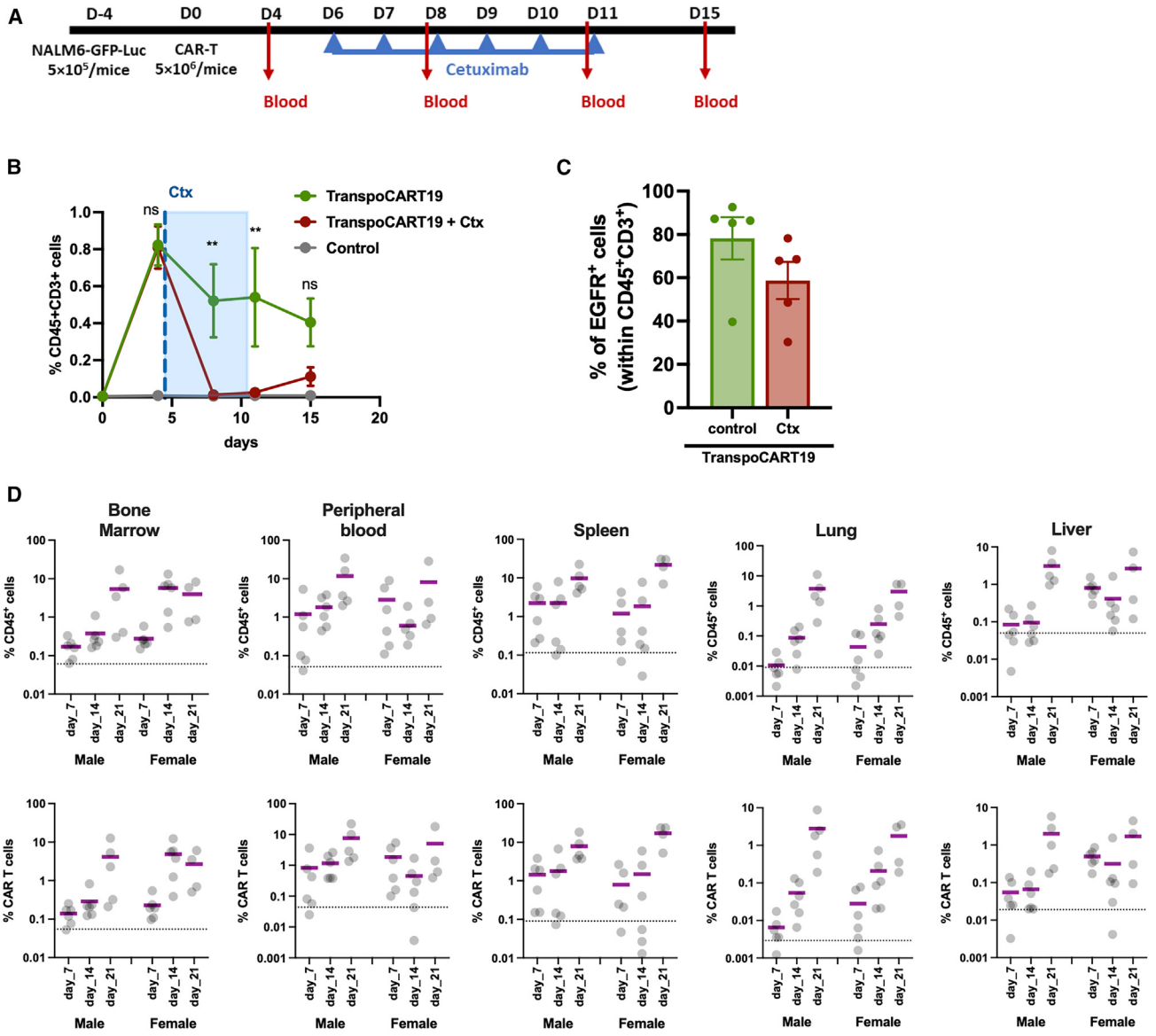

Figure 6. Evaluation of safety switch and biodistribution studies in TranspoCART19 cells

(A) Schematic representation of the experimental design to evaluate hEGFRt as a safety switch. Sub-lethally irradiated animals were transplanted with 10^6 NALM6 cells, and 4 days later animals were treated with 5×10^6 TranspoCART19 cells. Cetuximab (1 mg/mouse) was administered from day 6 to day 11. (B) Quantification of human $CD45^+CD3^+$ cells in blood samples obtained from treated animals on days 4, 8, 11, and 15 after TranspoCART19 cell administration. As controls, animals treated with PBS were included. (C) Quantification of the percentage of $hEGFRt^+$ cells within the $CD45^+CD3^+$ cells in blood samples obtained from animals treated with cetuximab or control IgG1 on day 15 after TranspoCART19 cell administration. (D) Quantification of human $CD45^+$ (upper panel) and $EGFR^+$ cells (lower panel) in different organs (bone marrow, peripheral blood, spleen, lung, and liver) of male and female animals (n = 4–6) treated with TranspoCART19 cells at different time points (days 7, 14, and 21). Mean ± SD is represented. Mixed effect model (REML) with Tukey's multiple comparisons test (B). ns: not significant; $^*p < 0.05$; $^{**}p < 0.01$, $^{***}p < 0.001$.

in a final volume of 30 mL using CryoMACS Freezing bags 250 (Miltenyi Biotech) containing saline, 10% DMSO, and 10% human albumin. Cryopreservation was carried out using IceCube 14M MED controlled freezer (Sy-Lab) using the following freezing curve: 4°C 20 min, 0.7°C 4 s, −10°C 10 min and 8 s, −55°C 51 s, −20°C 8 min and 59 s, −40°C 15 min, −60°C 10 min, and −120°C 5 min. Immediately after cryopreservation, freezing bags with the cells were stored at ≤ −120°C.

Flow cytometry

Phenotypic characterization of T cells and CAR-T cells was performed by flow cytometry. Cells were stained with several panels of

eight color combinations for 15 min at room temperature in the dark. Then cells were washed and acquired a BD FACSCanto II (BD Biosciences) or BD LSRFortessa cell analyzer (BD Biosciences) using FACS DIVA version 6.1 Software (Becton Dickinson). Data were analyzed using the FlowJo Software version 10. All antibodies were purchased from Biolegend unless otherwise stated (Table S1).

Cytotoxicity assay

The cytotoxic ability of CAR-T cells was determined using NALM6-GFPLuc, K562-GFPLuc, or K562-CD19-GFP-Luc cell lines as target cells. Briefly, target cells were cultured with CAR-T cells at different ratios in RPMI 1640 culture medium, supplemented with 3% human serum (Sigma) and 1% penicillin/streptomycin in Nunc 96-well round bottom plates (Thermo Fisher Scientific). Untransduced T cells (UTD) were used as control in some experiments. Luminescence was measured 24 h after coculture, using Bright-Glo Luciferase Assay System (Promega) according to the manufacturer's instructions. In some experiments, cytotoxicity was evaluated by flow cytometry. In this case, co-cultures were performed as described above, and the number of remaining live GFP^+ tumor cells was analyzed by flow cytometry in Troucount tubes according to the following formula: % of live cells = 100 × (number of GFP^+ cells with T cells/number of GFP^+ cells alone). Data were acquired on a BD FACSCanto II (BD Biosciences) using FACS DIVA versión 6.1 Software (Becton Dickinson) and analyzed using the FlowJo Software version 10.

Cytokine production

Cytokine production was measured in the supernatant of CAR-T:target cell co-cultures using BD LSRFortessa cell analyzer (BD Biosciences) using FACS DIVA version 6.1 Software (Becton Dickinson) and a Legend Plex HU Essential Immune Response Panel following the manufacturer's instructions. Results were analyzed using LEGENDplex v8.0 software. For some experiments, IFNγ, IL-2, and TNFα production was quantified using BD Immunoassay ELISA reagents (BD Biosciences) following manufacturer protocol.

Sleeping Beauty copy number analysis

Vector copy number (VCN) were determined by digital droplet PCR (ddPCR). Genomic DNA was extracted from TranspoCART19 cells using the DNeasy Blood and Tissue Kit (Qiagen). Then, 200 ng of DNA was digested overnight with 20 U of DpnI restriction enzyme (NEB) to eliminate non-integrated transposon minicircle present in the sample. Subsequently, the same DNA was digested 4 h using 20 U of CviQI restriction enzyme (NEB). Then, samples were amplified by PCR using TaqMan probes and primers specific for the repeat and inverted region and the right promoter of the transposon and the human reference gene RPP30 (Table S2). First, droplets are generated with the Bio-Rad automatic droplet generator. PCR is carried out in the Bio-Rad C100 Touch thermocycler in a 20 μL final volume with 10 ng of fragmented genomic DNA using ddPCR Supermix for probes (no dUTP) master mix (Bio-Rad) with 900 nM of primers and 250 nM of TaqMan probes. The PCR amplification protocol was: 10 min at 95°C, 40 cycles of 30 s at 94°C, 30 s at 56°C and 1 min at 72°C, followed by a final cycle of 5 min at 72°C and 10 min at 98°C. Once the amplification is completed, the fluorescent droplets were counted in the Bio-Rad QX200 droplet reader and genomic coy numbers were calculated with the QX Manager 1.2 program (Bio-Rad).

Integration site analysis

Integration site analysis (ISA) was performed on genomic DNA isolated with NucleoSpin Tissue for DNA extraction kit (Macherey-Nagel) from different TranspoCART19 cells generated by either LV-, or SB-mediated transgenesis. The conditions for genomic DNA ultra-sonication, adaptor ligation, and nested PCR-based library preparation (including primer sequences) for SB and LV vectors and the accompanying bioinformatic analyses have been described in detail.[18,33] The libraries containing the vector-genome junctions were sequencing using an Illumina NextSeq550 instrument with 1 × 150 bp setting. The raw sequence reads were quality, minimum-length and adapter trimmed using *fastp*.[34] The reads were mapped to the hg38 human genome assembly using *bowtie2*[35] with *–sensitive, --end-to-end* setting. We used *samtools*[36] to obtain "unique" mappers by applying the filter to the MAPQ values, which had to be any of 23, 24, 40, 42. The number of supporting reads per insertion site was calculated by the *genomecov* functions of *bedtools*.[37] Any suggested insertion site was accepted if the number of supporting reads were >10. We used the RefSeq annotations retrieved by the Table Browser application of the UCSC Genome Browser (https://genome-euro.ucsc.edu/) to obtain the coordinates of the gene related categories. The coordinates of the genomic safe harbors were created based on the RefSeq annotations above using the criteria proposed earlier.[38] The list of cancer genes was obtained from http://www.bushmanlab.or/lingks/genelists. The downstream analyses were performed using the *R* environment version 4.4 (https://www.r-project.org/). The sequence logos were plotted using the *seqLogo* package. The comparisons of insertion frequencies were done using four sets of 100,000 computationally generated random genomic locations, each. Student's t test was used to calculate *p* values when comparing insertion site frequencies between the conditions. The list of the insertion sites for the hg38 human genome assembly are provided as supplementary files (Table S3).

In vivo experiments

All experimental procedures were approved by the Ethics Committee of the University of Navarra and the Institute of Public Health of Navarra according to European Council Guidelines. NOD-SCID-gamma, NOD.Cg-Prkdcscid Il2rgtm1Wjl/SzJ (NSG) mice (The Jackson Laboratory) were bred and maintained in-house in a pathogen-free facility. Eight- to 12-week-old male or female mice were irradiated at 1.5 Gy at day 0 and 1 × 10^6 NALM6-GFPLuc cells were intravenously injected at day 1. Mice were randomized to ensure equal pre-treatment tumor burden before CAR-T cell treatment. At day 4, mice received intravenous injection of 3 × 10^6 CAR-T cells, 3 × 10^6 of UTD cells, or PBS. Tumor progression was measured by bioluminescent imaging using the PhotonIMAGER (Biospace Lab). Signal was quantified using M3Vision Analysis Software (Biospace Lab). Mice were humanely euthanized when mice demonstrated signs of morbidity and/or

hindlimb paralysis. To evaluate the efficacy of hEGFRt as a safety switch, NSG mice injected with NALM6-GFP-Luc tumor cells (10^6 cells/mouse) were treated with 5×10^6 CAR-T cells/mouse on day 4. Cetuximab or IgG1 control antibody (1 mg/mouse) were administered intraperitoneally every day from day 6 to 11. Blood was obtained on day 4 (before cetuximab administration), day 8 (48h after cetuximab administration), day 11 (5 days after cetuximab administration), and day 15 (4 days after cetuximab withdrawal) to measure the number of human $CD45^+CD3^+$ cells in peripheral blood by flow cytometry. Data were acquired on a BD FACSCanto II (BD Biosciences) using FACS DIVA version 6.1 Software (Becton Dickinson) and analyzed using the FlowJo Software version 10. For the biodistribution studies, female and male NSG mice were treated with 5×10^6 CAR-T cells/mouse 3 days after administration of 1×10^6 NALM6-GFP-Luc cells/mouse. As control, animals treated with PBS were included. On days 7, 14, and 21, animals were euthanized, and different organs/tissues were obtained (blood, bone marrow, spleen, liver, and lung). The presence of human hematopoietic cells ($CD45^+$) and CAR-T cells was determined by flow cytometry as described above.

Statistical analysis

Statistical analyses were performed using GraphPad Prism for Mac version 10.3.1. The different tests used in this work are indicated in the figure legend.

DATA AVAILABILITY

All data needed to evaluate the conclusions in the paper are present in the manuscript and/or the supplemental information. All data is available upon reasonable request form the corresponding authors.

ACKNOWLEDGMENTS

We particularly acknowledge the patients and healthy donors for their participation in this study, and the Biobank of the University of Navarra for its collaboration. This study was supported by the Instituto de Salud Carlos III co-financed by European Regional Development Fund-FEDER "A way to make Europe" (ICI19/00069, PT20/00163, PT23/00110 and PMPTA22/00109); Red de Terapia Celular TERCEL (RD16/0011/0005, RD16/0011/0015) and Red de Terapias Avanzadas TERAV (RD21/0017/0006, RD21/0017/0009 and RD21/0017/0027); Centro de Investigación Biomédica en Red de Cancer CIBERONC (CB16/12/00233, CB16/12/00489) and Centro de Investigación Biomédica en Red de Enfermedades Raras CIBERER (CB06/07/0014); Ministerio de Ciencia e Innovación co-financed by European Regional Development Fund-FEDER "A way to make Europe" (PID2022-137914OB-I00) and NextGenerationEU/PRTR (PLEC2021-008094); European Commission (T2EVOLVE: H2020-JTI-IMI2-2019-18, Contract 945393); and Gobierno de Navarra (SOCRATHeS: 0011-1411-2022-000053 and 0011-1411-2022-000088; DIAMANTE: 0011-1411-2023-000105 and 0011-1411-2023-000074; and GN2023/08). Gerencia Regional de Salud de Castilla y León (GRS 2182/A/2020, GRS2393/A/21).

AUTHOR CONTRIBUTIONS

B.D.: formal analysis, investigation and writing original draft. C.Calvino: formal analysis, investigation, and writing original draft. J.R.R.-M.: Conceptualization, investigation, formal analysis, funding acquisition and writing original draft. M.F.-G.: formal analysis and investigation. P.R.-M.: formal analysis, investigation and writing original draft. S.R.-D.: formal analysis and investigation. R.M.-T.: formal analysis and investigation. C.Ceballos: resources. J.I.: resources. J.S.-L.: resources. C.M.: formal analysis and software. A.N.-B.: resources and investigation. L.L.-C.: resources, investigation and funding acquisition. P.L.: resources. M.R.: resources. F.S.-G.: resources, investigation and funding acquisition. J.R.: resources and investigation. A.A.-P.: resources and investigation. Z.I.: resources and investigation. S.I.: formal analysis, investigation and writing original draft. A.L.-D.d.C.: formal analysis, investigation and writing original draft. R.Y.: formal analysis, investigation and writing original draft. J.A.B.: Conceptualization, investigation, funding acquisition and writing original draft. F.P.: Conceptualization, investigation, funding acquisition, and writing original draft.

DECLARATION OF INTERESTS

Z.I. is an inventor on patents related to Sleeping Beauty and MC technology.

SUPPLEMENTAL INFORMATION

Supplemental information can be found online at https://doi.org/10.1016/j.omtm.2025.101425.

REFERENCES

1. Jackson, H.J., Rafiq, S., and Brentjens, R.J. (2016). Driving CAR T-cells forward. Nat. Rev. Clin. Oncol. *13*, 370–383. https://doi.org/10.1038/nrclinonc.2016.36.

2. Neelapu, S.S., Locke, F.L., Bartlett, N.L., Lekakis, L.J., Miklos, D.B., Jacobson, C.A., Braunschweig, I., Oluwole, O.O., Siddiqi, T., Lin, Y., et al. (2017). Axicabtagene Ciloleucel CAR T-Cell Therapy in Refractory Large B-Cell Lymphoma. N. Engl. J. Med. *377*, 2531–2544. https://doi.org/10.1056/nejmoa1707447.

3. Schuster, S.J., Bishop, M.R., Tam, C.S., Waller, E.K., Borchmann, P., McGuirk, J.P., Jäger, U., Jaglowski, S., Andreadis, C., Westin, J.R., et al. (2019). Tisagenlecleucel in adult relapsed or refractory diffuse large B-cell lymphoma. N. Engl. J. Med. *380*, 45–56. https://doi.org/10.1056/NEJMoa1804980.

4. Maude, S.L., Laetsch, T.W., Buechner, J., Rives, S., Boyer, M., Bittencourt, H., Bader, P., Verneris, M.R., Stefanski, H.E., Myers, G.D., et al. (2018). Tisagenlecleucel in children and young adults with B-cell lymphoblastic leukemia. N. Engl. J. Med. *378*, 439–448. https://doi.org/10.1056/NEJMoa1709866.

5. Fowler, N.H., Dickinson, M., Dreyling, M., Martinez-Lopez, J., Kolstad, A., Butler, J., Ghosh, M., Popplewell, L., Chavez, J.C., Bachy, E., et al. (2022). Tisagenlecleucel in adult relapsed or refractory follicular lymphoma: the phase 2 ELARA trial. Nat. Med. *28*, 325–332. https://doi.org/10.1038/s41591-021-01622-0.

6. Wang, M., Munoz, J., Goy, A., Locke, F.L., Jacobson, C.A., Hill, B.T., Timmerman, J.M., Holmes, H., Jaglowski, S., Flinn, I.W., et al. (2020). KTE-X19 CAR T-Cell therapy in relapsed or refractory mantle-cell lymphoma. N. Engl. J. Med. *382*, 1331–1342. https://doi.org/10.1056/NEJMoa1914347.

7. Munshi, N.C., Anderson, L.D., Shah, N., Madduri, D., Berdeja, J., Lonial, S., Raje, N., Lin, Y., Siegel, D., Oriol, A., et al. (2021). Idecabtagene Vicleucel in Relapsed and Refractory Multiple Myeloma. N. Engl. J. Med. *384*, 705–716. https://doi.org/10.1056/NEJMoa2024850.

8. Berdeja, J.G., Madduri, D., Usmani, S.Z., Jakubowiak, A., Agha, M., Cohen, A.D., Stewart, A.K., Hari, P., Htut, M., Lesokhin, A., et al. (2021). Ciltacabtagene autoleucel, a B-cell maturation antigen-directed chimeric antigen receptor T-cell therapy in patients with relapsed or refractory multiple myeloma (CARTITUDE-1): a phase 1b/2 open-label study. Lancet *398*, 314–324. https://doi.org/10.1016/S0140-6736(21)00933-8.

9. Abramson, J.S., Palomba, M.L., Gordon, L.I., Lunning, M.A., Wang, M., Arnason, J., Mehta, A., Purev, E., Maloney, D.G., Andreadis, C., et al. (2020). Lisocabtagene maraleucel for patients with relapsed or refractory large B-cell lymphomas (TRANSCEND NHL 001): a multicentre seamless design study. Lancet *396*, 839–852. https://doi.org/10.1016/S0140-6736(20)31366-0.

10. Shah, N.N., Qin, H., Yates, B., Su, L., Shalabi, H., Raffeld, M., Ahlman, M.A., Stetler-Stevenson, M., Yuan, C., Guo, S., et al. (2019). Clonal expansion of CAR T cells harboring lentivector integration in the CBL gene following anti-CD22 CAR T-cell therapy. Blood Adv. *3*, 2317–2322. https://doi.org/10.1182/bloodadvances.2019000219.

11. Micklethwaite, K.P., Gowrishankar, K., Gloss, B.S., Li, Z., Street, J.A., Moezzi, L., Mach, M.A., Sutrave, G., Clancy, L.E., Bishop, D.C., et al. (2021). Investigation of product-derived lymphoma following infusion of piggyBac-modified CD19 chimeric antigen receptor T cells. Blood *138*, 1391–1405. https://doi.org/10.1182/blood.2021010858.

12. Bishop, D.C., Clancy, L.E., Simms, R., Burgess, J., Mathew, G., Moezzi, L., Street, J.A., Sutrave, G., Atkins, E., McGuire, H.M., et al. (2021). Development of CAR T-cell

lymphoma in 2 of 10 patients effectively treated with piggyBac-modified CD19 CAR T cells. Blood *138*, 1504–1509. https://doi.org/10.1182/blood.2021010813.

13. Schambach, A., Morgan, M., and Fehse, B. (2021). Two cases of T cell lymphoma following Piggybac-mediated CAR T cell therapy. Mol. Ther. *29*, 2631–2633. https://doi.org/10.1016/j.ymthe.2021.08.013.
14. Cliff, E.R.S., Kelkar, A.H., Russler-Germain, D.A., Tessema, F.A., Raymakers, A.J.N., Feldman, W.B., and Kesselheim, A.S. (2023). High Cost of Chimeric Antigen Receptor T-Cells: Challenges and Solutions (American Society of Clinical Oncology Educational Book). https://doi.org/10.1200/edbk_397912.
15. Irving, M., Lanitis, E., Migliorini, D., Ivics, Z., and Guedan, S. (2021). Choosing the Right Tool for Genetic Engineering: Clinical Lessons from Chimeric Antigen Receptor-T Cells. Hum. Gene Ther. *32*, 1044–1058. https://doi.org/10.1089/hum.2021.173.
16. Izsvák, Z., and Ivics, Z. (2004). Sleeping Beauty transposition: Biology and applications for molecular therapy. Mol. Ther. *9*, 147–156. https://doi.org/10.1016/j.ymthe.2003.11.009.
17. Galvan, D.L., Nakazawa, Y., Kaja, A., Kettlun, C., Cooper, L.J.N., Rooney, C.M., and Wilson, M.H. (2009). Genome-wide mapping of piggybac transposon integrations in primary human T cells. J. Immunother. *32*, 837–844. https://doi.org/10.1097/CJI.0b013e3181b2914c.
18. Miskey, C., Kesselring, L., Querques, I., Abrusán, G., Barabas, O., and Ivics, Z. (2022). Engineered Sleeping Beauty transposase redirects transposon integration away from genes. Nucleic Acids Res. *50*, 2807–2825. https://doi.org/10.1093/nar/gkac092.
19. Miskey, C., Amberger, M., Reiser, M., Prommersberger, S., Beckmann, J., Machwirth, M., Einsele, H., Hudecek, M., Bonig, H., and Ivics, Z. (2019). Genomic Analyses of SLAMF7 CAR-T Cells Manufactured by Sleeping Beauty Transposon Gene Transfer for Immunotherapy of Multiple Myeloma. Preprint at bioRxiv. https://doi.org/10.1101/675009.
20. Gogol-Doring, A., Ammar, I., Gupta, S., Bunse, M., Miskey, C., Chen, W., Uckert, W., Schulz, T.F., Izsvak, Z., and Ivics, Z. (2016). Genome-wide profiling reveals remarkable parallels between insertion site selection properties of the MLV retrovirus and the piggyBac transposon in primary human CD4+ T cells. Mol. Ther. *24*, 595–606. https://doi.org/10.1038/mt.2016.11.
21. Monjezi, R., Miskey, C., Gogishvili, T., Schleef, M., Schmeer, M., Einsele, H., Ivics, Z., and Hudecek, M. (2017). Enhanced CAR T-cell engineering using non-viral Sleeping Beauty transposition from minicircle vectors. Leukemia *31*, 186–194. https://doi.org/10.1038/leu.2016.180.
22. Calviño, C., Ceballos, C., Alfonso, A., Jauregui, P., Calleja-cervantes, M.E., Martin-uriz, P.S., Rodriguez-Marquez, P., Rodriguez-Diaz, S., Martinez-turrillas, R., Illarramendi, J., et al. (2023). Optimization of universal allogeneic CAR-T cells combining CRISPR and transposon-based technologies for treatment of acute myeloid leukemia. Front. Immunol. *14*, 1–16. https://doi.org/10.3389/fimmu.2023.1270843.
23. Rodriguez-Marquez, P., Calleja-Cervantes, M.E., Serrano, G., Oliver-Caldes, A., Palacios-Berraquero, M.L., Martin-Mallo, A., Calviño, C., Español-Rego, M., Ceballos, C., Lozano, T., et al. (2022). CAR Density Influences Antitumoral Efficacy of BCMA CAR T cells and Correlates with Clinical Outcome. Sci. Adv. *2022*, 22269515. https://doi.org/10.1101/2022.01.19.22269515.
24. Prommersberger, S., Reiser, M., Beckmann, J., Danhof, S., Amberger, M., Quade-Lyssy, P., Einsele, H., Hudecek, M., Bonig, H., and Ivics, Z. (2021). CARAMBA: a first-in-human clinical trial with SLAMF7 CAR-T cells prepared by virus-free Sleeping Beauty gene transfer to treat multiple myeloma. Gene Ther. *28*, 560–571. https://doi.org/10.1038/s41434-021-00254-w.
25. Singh, H., Srour, S.A., Milton, D.R., McCarty, J., Dai, C., Gaballa, M.R., Ammari, M., Olivares, S., Huls, H., De Groot, E., et al. (2022). Sleeping beauty generated CD19 CAR T-Cell therapy for advanced B-Cell hematological malignancies. Front. Immunol. *13*, 1032397. https://doi.org/10.3389/fimmu.2022.1032397.
26. Prommersberger, S., Jetani, H., Danhof, S., Monjezi, R., Nerreter, T., Beckmann, J., Einsele, H., and Hudecek, M. (2018). Novel targets and technologies for CAR-T cells in multiple myeloma and acute myeloid leukemia. Curr. Res. Transl. Med. *66*, 37–38. https://doi.org/10.1016/j.retram.2018.03.006.
27. Magnani, C.F., Gaipa, G., Lussana, F., Belotti, D., Gritti, G., Napolitano, S., Matera, G., Cabiati, B., Buracchi, C., Borleri, G., et al. (2020). Sleeping Beauty–engineered CAR T cells achieve antileukemic activity without severe toxicities. J. Clin. Investig. *130*, 6021–6033. https://doi.org/10.1172/JCI138473.
28. Tipanee, J., Samara-Kuko, E., Gevaert, T., Chuah, M.K., and VandenDriessche, T. (2022). Universal allogeneic CAR T cells engineered with Sleeping Beauty transposons and CRISPR-CAS9 for cancer immunotherapy. Mol. Ther. *30*, 3155–3175. https://doi.org/10.1016/j.ymthe.2022.06.006.
29. Melenhorst, J.J., and Oliveira, B.C. (2024). Key role of CD4+ T cells in determining CD8 function during CAR-T cell manufacture. J. Immunother. Cancer. *12*, e008723. https://doi.org/10.1136/jitc-2023-008723.
30. Melenhorst, J.J., Chen, G.M., Wang, M., Porter, D.L., Chen, C., Collins, M.A., Gao, P., Bandyopadhyay, S., Sun, H., Zhao, Z., et al. (2022). Decade-long leukaemia remissions with persistence of CD4+ CAR T cells. Nature *602*, 503–509. https://doi.org/10.1038/s41586-021-04390-6.
31. Galli, E., Bellesi, S., Pansini, I., Di Cesare, G., Iacovelli, C., Malafronte, R., Maiolo, E., Chiusolo, P., Sica, S., Sorà, F., and Hohaus, S. (2023). The CD4/CD8 ratio of infused CD19-CAR-T is a prognostic factor for efficacy and toxicity. Br. J. Haematol. *203*, 564–570. https://doi.org/10.1111/bjh.19117.
32. Wang, X., Chang, W.C., Wong, C.W., Colcher, D., Sherman, M., Ostberg, J.R., Forman, S.J., Riddell, S.R., and Jensen, M.C. (2011). A transgene-encoded cell surface polypeptide for selection, *in vivo* tracking, and ablation of engineered cells. Blood *118*, 1255–1263. https://doi.org/10.1182/blood-2011-02-337360.
33. Bexte, T., Botezatu, L., Miskey, C., Gierschek, F., Moter, A., Wendel, P., Reindl, L.M., Campe, J., Villena-Ossa, J.F., Gebel, V., et al. (2024). Engineering of potent CAR NK cells using non-viral Sleeping Beauty transposition from minimalistic DNA vectors. Mol. Ther. *32*, 2357–2372. https://doi.org/10.1016/j.ymthe.2024.05.022.
34. Chen, S., Zhou, Y., Chen, Y., and Gu, J. (2018). Fastp: An ultra-fast all-in-one FASTQ preprocessor. Bioinformatics *34*, i884–i890. https://doi.org/10.1093/bioinformatics/bty560.
35. Langmead, B., and Salzberg, S.L. (2012). Fast gapped-read alignment with Bowtie 2. Nat. Methods *9*, 357–359. https://doi.org/10.1038/nmeth.1923.
36. Li, H., Handsaker, B., Wysoker, A., Fennell, T., Ruan, J., Homer, N., Marth, G., Abecasis, G., and Durbin, R.; 1000 Genome Project Data Processing Subgroup (2009). The Sequence Alignment/Map format and SAMtools. Bioinformatics *25*, 2078–2079. https://doi.org/10.1093/bioinformatics/btp352.
37. Quinlan, A.R., and Hall, I.M. (2010). BEDTools: A flexible suite of utilities for comparing genomic features. Bioinformatics *26*, 841–842. https://doi.org/10.1093/bioinformatics/btq033.
38. Sadelain, M., Papapetrou, E.P., and Bushman, F.D. (2012). Safe harbours for the integration of new DNA in the human genome. Nat. Rev. Cancer *12*, 51–58. https://doi.org/10.1038/nrc3179.